Am. J. Hum. Genet. 68:1077–1085, 2001

Identification and Expression Analysis of Spastin Gene Mutations in Hereditary Spastic Paraplegia

Ingrid K. Svenson,[1] Allison E. Ashley-Koch,[1] P. Craig Gaskell,[1] Travis J. Riney,[1] W. J. Ken Cumming,[2] Helen M. Kingston,[3] Edward L. Hogan,[4] Rose-Mary N. Boustany,[1] Jeffery M. Vance,[1] Martha A. Nance,[5] Margaret A. Pericak-Vance,[1] and Douglas A. Marchuk[1]

[1]Duke University Medical Center, Durham, NC; [2]Neuroscience Unit, The Alexandria Hospital, Cheshire, United Kingdom; [3]Regional Genetic Service, St. Mary's Hospital, Manchester, United Kingdom; [4]Medical University of South Carolina, Charleston; and [5]Park Nicollet Clinic, Minneapolis

Pure hereditary spastic paraplegia (SPG) type 4 is the most common form of autosomal dominant hereditary SPG, a neurodegenerative disease characterized primarily by hyperreflexia and progressive spasticity of the lower limbs. It is caused by mutations in the gene encoding spastin, a member of the AAA family of ATPases. We have screened the spastin gene for mutations in 15 families consistent with linkage to the spastin gene locus, *SPG4*, and have identified 11 mutations, 10 of which are novel. Five of the mutations identified are in noninvariant splice-junction sequences. Reverse transcription–PCR analysis of mRNA from patients shows that each of these five mutations results in aberrant splicing. One mutation was found to be "leaky," or partially penetrant; that is, the mutant allele produced both mutant (skipped exon) and wild-type (full-length) transcripts. This phenomenon was reproduced in in vitro splicing experiments, with a minigene splicing-vector construct only in the context of the endogenous splice junctions flanking the splice junctions of the skipped exon. In the absence of endogenous splice junctions, only mutant transcript was detected. The existence of at least one leaky mutation suggests that relatively small differences in the level of wild-type spastin expression can have significant functional consequences. This may account, at least in part, for the wide ranges in age at onset, symptom severity, and rate of symptom progression that have been reported to occur both among and within families with SPG linked to *SPG4*. In addition, these results suggest caution in the interpretation of data solely obtained with minigene constructs to study the effects of sequence variation on splicing. The lack of full genomic sequence context in these constructs can mask important functional consequences of the mutation.

Introduction

The hereditary spastic paraplegias (SPGs) are a genetically heterogeneous group of neurodegenerative disorders characterized by progressive lower-limb spasticity and hyperreflexia, occurring in the absence (pure SPG) or presence (complicated SPG) of other major clinical abnormalities, such as optic neuropathy, deafness, and mental retardation (Fink 1997). Neuropathologically, SPG is characterized by axonal degeneration that is maximal at the distal ends of the longest axons of the CNS (McDermott et al. 2000). The genetic heterogeneity of SPG is reflected by the fact that, to date, >12 SPG loci have been identified, including loci for pure and complicated autosomal dominant, autosomal recessive, and X-linked SPG.

Received January 16, 2001; accepted for publication March 14, 2001; electronically published April 16, 2001.

Address for correspondence and reprints: Dr. Douglas Marchuk, Box 3175, Duke University Medical Center, Durham, NC 27710. E-mail: march004@mc.duke.edu

0002-9297/2001/6805-0002$02.00

The most common form of autosomal dominant pure SPG (MIM 182601) is caused by mutations in the gene encoding spastin, a member of the AAA family of ATPases (Hazan et al. 1999). The members of this family are characterized by the presence of one or more highly conserved AAA motifs that contain Walker-homology domains and harbor the ATPase activity. The AAA ATPases are thought to act as molecular chaperones in the assembly, function, and disassembly of protein complexes and play essential roles in a wide variety of cellular activities, including protein degradation, vesicle-mediated protein transport, cell-cycle regulation, organelle biogenesis, and gene expression (Patel and Latterich 1998; Neuwald et al. 1999).

The >40 spastin gene mutations described to date include missense, nonsense, and splice-site point mutations, as well as insertions and deletions, and almost all seem to affect, either directly or indirectly, the AAA motif–encoding region of the gene (Bürger et al. 2000; Fonknechten et al. 2000; Hentati et al. 2000; Lindsey et al. 2000; Santorelli et al. 2000). In the present study, we screened the spastin gene for mutations in the probands of 15 families with autosomal dominant pure

SPG and investigated the effects that some of these mutations have on splicing of the spastin gene transcript.

Families and Methods

Families

Informed consent, blood samples, and clinical evaluations were obtained from all participating family members, under protocols approved by institutional review boards. Fifteen families, some of whom have been described elsewhere (Scott et al. 1997), were included in the spastin gene mutation analysis; they are listed in table 1, together with the maximum expected LOD score and maximum LOD score calculated for each family at *SPG4*-linked marker *D2S352* or *D2S367*. The maximum expected LOD scores were calculated with SIMLINK (Boehnke 1986; Ploughman and Boehnke 1989), under the assumptions of an autosomal dominant model with age-dependent penetrance, a disease-allele frequency of .001, and a marker with four alleles, at frequencies .40, .30, .20, and .10. For each family, 1,000 replicates were generated. Age at onset was defined either as the age at which the individual reported awareness of a significant change in gait pattern or as the age at which a parent noted awkward gait or change in gait in a child.

Mutation Detection

Each exon and flanking intronic sequence of the spastin gene was amplified by PCR, from 100 ng of genomic DNA extracted from peripheral blood samples from an affected individual of each family. The sequences of the primers and the conditions for PCR amplification have been described elsewhere (by Genoscope Centre National de Séquençage and Hazan et al. [1999], respectively). The PCR products were run on 1% Agarose II (Amresco), run on 0.5% Tris-borate EDTA (TBE) gels, eluted from the gel by freezing and then centrifuging at 18,000 *g* for 10 min, and sequenced with the Thermo Sequenase Radiolabeled Terminator Cycle Sequencing Kit (USB). Potential mutations were tested for cosegregation with the disease phenotype and were screened for in $\geqslant$100 population-control individuals, by either restriction enzyme digestion or conformation sensitive gel electrophoresis (Körkkö et al. 1998).

mRNA Expression Studies

Total RNA was extracted from patient lymphoblastoid cell lines or patient peripheral blood samples (as available) or from normal human brain and was used as a template for cDNA synthesis with random hexamer and oligo dT_{15} primers and 200 U of Moloney murine leukemia virus (M-MLV) reverse transcriptase (Life Technologies), according to standard procedures. PCR products amplified from the cDNA samples were run on

Table 1

Summary of Family Data and Mutations Identified

Mutation			Family (No. of Affected Individuals)	Expected/ Observed Maximum LOD Score	Average Age at Onset [Range] (Years)
Type[a]	Location	Consequence			
Nonsense/frameshift:					
465G→T	Exon 1	Stop codon (E114X)	1890 (4)	1.1/1.47	47 [39–62]
1486insA	Exon 11	Frameshift	1939 (10)	4.1/4.47	35.5 [20–45]
Missense:					
1620C→T	Exon 13	R499C	2182 (4)	2.2/1.92	24.5 [3–40]
1809C→G	Exon 15	R562G	1380 (11)	2/3.34	24.5 [1–40]
Invariant (GT–––AG) splice-site sequence:					
IVS9+1G→A	Intron 9	Skipped exon 9	1974 (4)	.9/.75	34.8 [20–50]
IVS12−2A→C	Intron 12	Skipped exon 13	1858 (6)	1.1/1.09	37.8 [1–59]
Others that affect splicing:					
995G→T	Exon 5	Exon 5 skipping; K290N	1713 (10)	3.2/2.09	30.8 [18–46]
1367A→G	Exon 9	4-nt deletion from 3′ end of exon 9 (K414K)	1676 (7)	3.2/1.64	36.7 [23–43]
IVS9+4A→G	Intron 9	Exon 9 skipping	1838 (12)	3.8/3.82	32.2 [2–56]
IVS9+6T→G	Intron 9	Exon 9 skipping	2082 (8)	3.3/2.47	25.1 [10–36]
IVS11+2insT	Intron 11	Exon 11 skipping	2187 (6)	1.3/1.32	30.8 [5–40]
None detected:					
…	…	…	1806 (3)	1.9/1.23	56.5 [42–71]
…	…	…	1884 (4)	.8/.86	22 [4–32]
…	…	…	1891 (5)	.9/1.35	24 [18–28]
…	…	…	1985 (5)	.9/.6	31 [20–48]

[a] Nucleotide numbering is that used by Genoscope Centre National de Séquençage.

1% Agarose II, run on 0.5% TBE gels, and sequenced as described above.

Subcloning and Transfection Experiments

PCR products spanning exon 5, exon 9, exons 10–12, and exons 8–12, each with ⩾100 bp of flanking intronic sequence, were amplified from patient genomic DNA. The primers used were SPAex5a, SPAex5m, SPGex8a, SPAex9a, SPAex9m, SPAex10a, and SPAex12m (Genoscope Centre National de Séquençage), each with an *Eco*RI or a *Bam*HI restriction enzyme cleavage site–compatible tail. These PCR products were cloned into pSPL3 (Exon Trapping System; Life Technologies) and then sequenced. Clones with or without the mutation of interest, as well as the vector alone, were transfected into COS1 cells, by use of Lipofectamine (Life Technologies), according to the manufacturer's instructions. Cytoplasmic RNA was isolated from the transfected cells after 36 h and then used as a template for cDNA synthesis, with vector-specific primer SA2 (ATCTCAGTGGTATTTGTGAGC; Exon Trapping System) and 200 U of M-MLV reverse transcriptase, according to the manufacturer's instructions. PCR products amplified from the cDNA samples with vector-specific primers SD6 (TCTGAGTCACCTGGACAACC) and SA2 or exon-specific primers, were run on 1% Agarose II, run on 0.5% TBE gels, and sequenced as described above.

Results

Mutation Detection

In 11 of the 15 families screened (table 1), we identified spastin gene mutations, 10 of which were novel. One missense mutation, 1620C→T (R499C), has been described elsewhere (Hazan et al. 1999), and it should be noted that this C→T transition occurs at a CpG dinucleotide. Figure 1 shows a schematic of the spastin cDNA and the positions of the mutations identified in this study. In addition to one nonsense mutation, one frameshift mutation, and two missense-only mutations, we identified seven mutations that affect splicing, one of which is also a missense mutation (995G→T [K290N]; fig. 2). We found no obvious relationship between the type or location of the mutations and the age at onset of symptoms (table 1). The age at onset varied widely, both within and among the families, and the average age at onset did not differ markedly among the families.

The nonsense mutation that we identified, 465G→T, causes a change from a glutamic acid to a stop codon in exon 1. The frameshift mutation that we identified, 1486insA, occurs in exon 11, in the AAA cassette–encoding region of the gene. We identified three missense mutations, one of which also affects splicing. The 1620C→T and 1809C→G mutations both result in a nonconservative amino acid codon change—from, respectively, an arginine to a cysteine codon (R499C) in exon 13 and from an arginine to a glycine codon (R562G) in exon 15. Both of these arginine residues are located in the AAA cassette, and both are conserved among spastin homologs in yeast, *Caenorhabditis elegans,* and mice (Hazan et al. 1999). The third missense mutation, 995G→T (K290N), also results in a nonconservative amino acid codon change, from a lysine to an asparagine codon at the 3′ end of exon 5. This mutation also disrupts splicing: it causes skipping of exon 5, with a consequent frameshift, as demonstrated by reverse transcription–PCR (RT-PCR) analysis (fig. 2).

We identified seven mutations that affect splicing. Each

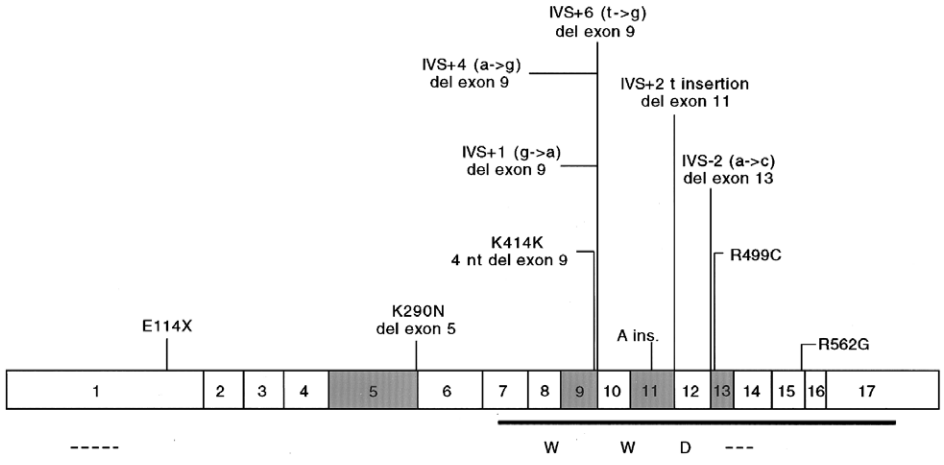

Figure 1 Schematic of spastin cDNA. The thicker horizontal black line indicates the AAA cassette–encoding region of the gene; the thinner, dashed lines indicate the leucine-zipper motif. The vertical lines indicate positions of mutations. Exons that are deleted as a result of splice-site mutations are shaded. W = Walker motif; D = dimerization domain.

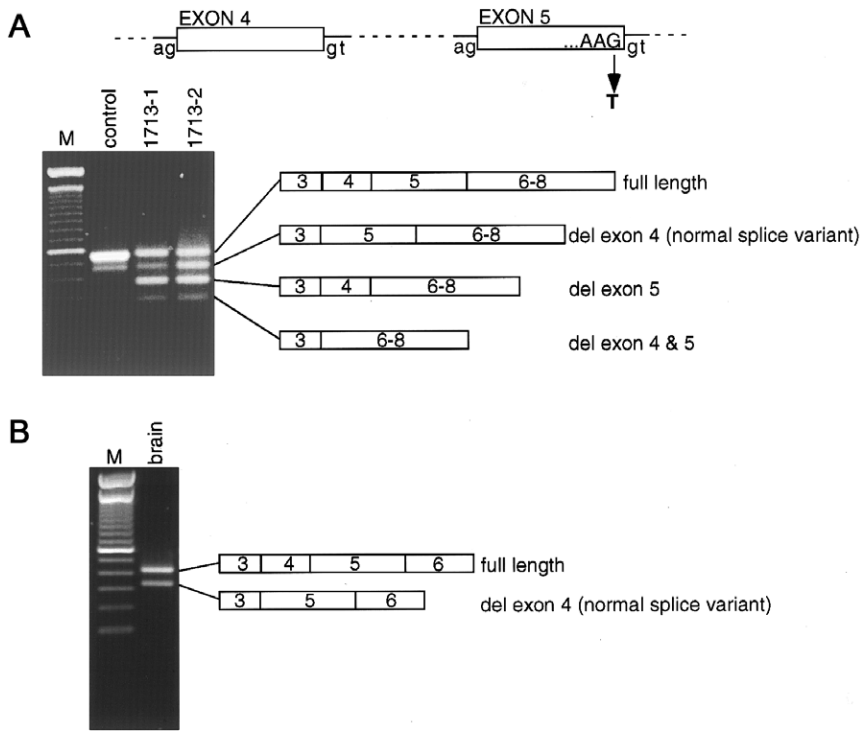

Figure 2 Aberrant splicing resulting from the 995G→T mutation. *A*, Schematic showing the position of the G995T mutation in family 1713 (*top*) and RT-PCR products from lymphocyte RNA from two affected individuals from family 1713 (*bottom*). For this and subsequent figures, the identity of each RT-PCR–product band was confirmed by DNA sequencing. The mutation causes skipping of exon 5. A normal splice variant missing exon 4 is found in samples from both control subjects and affected individuals. *B*, RT-PCR products showing the presence of the normal splice variant lacking exon 4, in RNA extracted from a sample of normal human brain tissue.

mutation either lies within the AAA cassette–encoding region of the gene or affects splicing of an exon in this region. Only two of the mutations are located in an invariant (GT–––AG) donor or acceptor splice-site sequence. The splice-acceptor–site mutation IVS12−2A→C causes skipping of exon 13 (fig. 3), and the splice-donor–site mutation IVS9+1G→A causes skipping of exon 9 (fig. 4). Both of these exons lie within the AAA cassette–encoding region of the gene.

The remaining five mutations that affect splicing are located outside the invariant (GT–––AG) splice-site sequences. Four of them—995G→T, IVS9+4A→G, IVS9+6T→G, and IVS11+2insT—result in skipping of an entire exon (figs. 2, 4, and 5). The fifth mutation, 1367A→G, results in the creation of a new splice-donor site 4 nt upstream of the 3′ end of exon 9, causing deletion of the last 4 nt of exon 9 (fig. 6).

We also detected one synonymous substitution, 1004G→A (P293P), in exon 6 in the proband of family 1838. This nucleotide change was found in a single individual in the youngest generation of the pedigree and was not found in 84 control individuals. To our knowledge, no other polymorphisms have been detected in a spastin gene coding exon.

mRNA Expression Studies

During the RT-PCR analysis of RNA isolated from lymphocytes, we identified three spastin mRNA splice variants, in both control and patient samples; we also identified these same variants in RNA extracted from a sample of normal human brain. In all cases, the splice variant, as visualized by gel electrophoresis, was less abundant than the full-length spastin transcript. Figure 2 shows skipping of exon 4 in both control and patient samples; this skipped exon is upstream of the AAA-cassette region, and the transcript retains the correct reading frame. Another normal splice variant lacks exon 8, which lies within the AAA-cassette region and includes the Walker A motif; this transcript also retains the correct reading frame. The third normal splice variant is missing exon 15, which also lies within the AAA-cassette region but downstream of the Walker A and B motifs, the helix-loop-helix dimerization domain, and the leucine-zipper motif. However, unlike skipping of exon 4 or exon 5, skipping of exon 15 causes a frameshift. All three of these splice variants were detected consistently, although, particularly in the case of the last two, at very low levels. After accounting for these normal splice var-

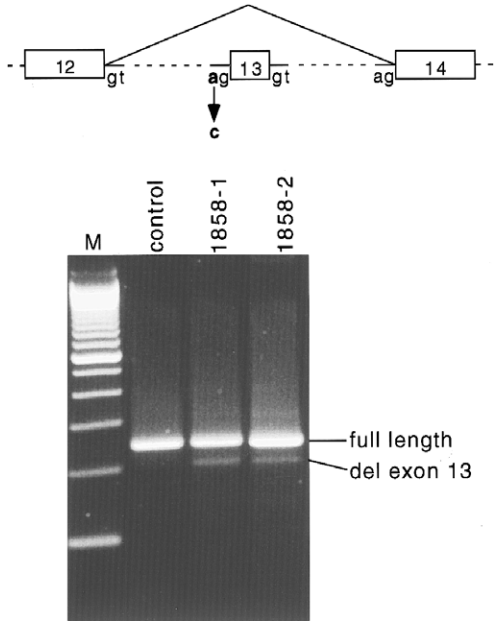

Figure 3 Aberrant splicing resulting from the IVS12−2A→C mutation. *Top,* Schematic showing the position of the IVS12−2A→C mutation in family 1858. *Bottom,* RT-PCR products from lymphocyte RNA from two affected individuals from family 1858. The mutation causes skipping of exon 13.

iants, we could easily interpret the results of our mRNA expression studies.

In four of the six splice-site–mutation cases for which patient-derived RNA was available for study, the aberrant-size transcript, as visualized by gel electrophoresis, was much less abundant than the wild-type transcript. This may indicate that the mutant transcript is either less stable or expressed at a lower level than is the wild-type transcript. Alternatively, these mutations may be "leaky," or not fully penetrant; that is, some normally spliced transcript may be produced from the mutant allele. In two cases, sequence variation within the transcript allowed us to test the latter possibility. In the case of the 995G→T mutation in exon 5, which also causes aberrant splicing (fig. 2), homozygosity was detected at position 995 (the site of the mutation) in the normally spliced transcript, indicating that normally spliced transcript was produced exclusively from the wild-type allele. In contrast, both aberrantly and normally spliced transcripts were produced from the allele with the IVS9+4A→G mutation (fig. 5*A*). To exclude any amplification of aberrantly spliced transcripts, we designed one of the amplification primers in exon 9, which is absent from the aberrantly spliced transcript. Subsequent sequencing of the full-length transcript, with either primer used in the amplification, revealed heterozygosity for the 1004G→A private polymorphism in exon 6 (fig. 5*B*). This indicates that the full-length, normally spliced transcript was produced from both the wild-type and the mutant allele in this patient.

Unfortunately, for the other splice-site mutations that we identified, no coding-region polymorphism was available to determine whether a given transcript was produced from the mutant or the wild-type allele. To determine whether any of the other splice-site mutations were leaky, we expressed them separately, in vitro, to examine their effect on splicing independent of the wild-type allele. We subcloned the mutations, with surrounding genomic sequence into an exon-trapping vector, pSPL3, and transfected these minigene constructs into COS1 cells, for mRNA expression studies. As shown in figure 7, none of the mutations—including the IVS9+4A→G mutation that we had found to be leaky in vivo—caused aberrant splicing in this in vitro system. However, in all but one of these cases, the construct contained only the exon affected by the mutation, along with flanking intronic sequence. To determine whether the leakiness of the IVS9+4A→G mutation would be

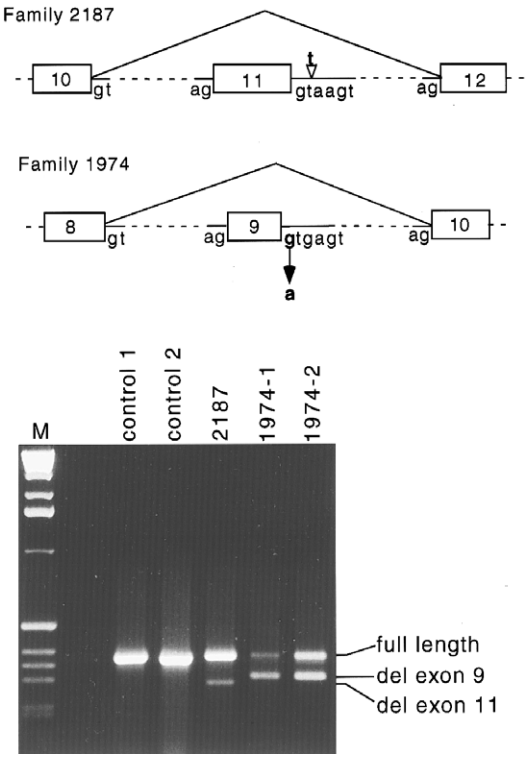

Figure 4 Aberrant splicing resulting from the IVS11+2T insertion and the IVS9+1G→A mutation. *Top,* Schematic showing the positions of the IVS11+2T insertion in family 2187 and of the IVS9+1G→A mutation in family 1974. *Bottom,* RT-PCR products from lymphocyte RNA from three affected individuals, one from family 2187 and two from family 1974. The mutation in family 2187 causes skipping of exon 11, and the mutation in family 1974 causes skipping of exon 9.

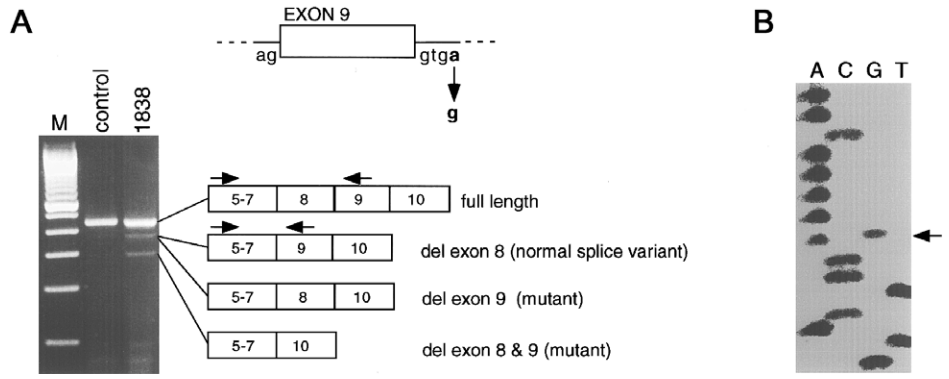

Figure 5 Aberrant splicing resulting from the leaky IVS9+4A→G mutation. *A,* Schematic showing the position of the IVS9+4A→G mutation in family 1838 (*top*) and RT-PCR products from lymphocyte RNA from an affected individual from family 1838 (*bottom*). The mutation causes skipping of exon 9. A normal splice variant missing exon 8 is reproducibly found in samples both from control subjects and from affected individuals. In this figure, it is barely visible in the control lane. In the lane for family 1838, the middle band represents both the mutant transcript missing exon 9 and the normal splice variant missing exon 8 and thus is more easily visible. *B,* Sequencing-gel autoradiograph showing heterozygosity for the 1004G→A private polymorphism in exon 6 in normally spliced transcript. RNA from lymphocytes from an affected individual from family 1838 was analyzed by RT-PCR. To prevent amplification of any contaminating mutant transcript, a reverse primer was chosen in exon 9, which is absent from the mutant transcript (for positions of primers, see *A*). The sequence of the normally spliced full-length transcript is heterozygous for the 1004G→A private polymorphism in exon 6 (*arrow*). This heterozygosity was present both in the sequence generated with the exon 5–specific primer (*shown*) and in sequence generated with the exon 9–specific primer.

reproduced in a more extensive genomic-sequence context in vitro, we used a minigene construct containing additional flanking exons and intronic sequence (fig. 8). In this sequence context, both full-length and mutant (missing exon 9) transcripts were produced from the mutant construct.

Discussion

Each of the four families in whom we found no spastin gene mutations was relatively small, with the maximum LOD score <1.5 for *SPG4*-linked markers. Although it is possible that these families harbor an undetected mutation either in the spastin gene or in one of its regulatory regions, it is also possible that they instead segregate a mutation either at one of the six other autosomal dominant SPG loci that have been identified to date or at an unidentified SPG locus (Fontaine et al. 2000; McDermott et al. 2000; Reid et al. 2000). A genomewide screen of these families for evidence of linkage to other loci is currently under way.

All of the mutations identified in this study are consistent with loss of spastin function, consistent with the previously described mutations. The importance of the AAA cassette in spastin function is suggested by its high degree of conservation among AAA protein family members and by the locations of the spastin gene mutations identified to date. The AAA cassette contains Walker A and B motifs (the putative sites of ATP binding and ATPase activity), a helix-loop-helix dimerization domain, and a leucine-zipper motif. All of the mutations identified in the present study are predicted to affect the AAA cassette, with all but one affecting one or more of the known motifs in this region; the lone exception, the 1809C→G mutation in exon 15, alters a highly conserved arginine residue within the AAA cassette. The region outside the AAA cassette is much less conserved among members of the very large family of AAA proteins (Patel and Latterich 1998). Nonetheless, at the amino acid level, human spastin is 96% identical to its mouse ortholog, throughout the protein. This high level of identity and the extremely low level of polymorphism throughout the coding exons of the spastin gene suggest a low level of tolerance for amino acid substitutions, throughout the protein. This is in contrast to the tolerance, at least to some extent, for variability at the level of spastin mRNA splicing. Two of the normal splice variants that we identified directly affect the AAA-cassette region of the protein. The functional significance of these splice variants is unclear, but their presence may suggest functions for spastin that are independent of the AAA cassette.

The majority of mutations that we identified create aberrant splice variants of the spastin transcript. Although our findings regarding the effects of the splice-site mutations were in lymphocytes, each of these mutations causes skipping of an exon that is otherwise included in all splice variants identified to date, including transcripts derived from brain RNA. Since these exons do not appear to be affected by alternative splicing, they should be processed by the splicing machinery common to all cell types. As such, these mutations

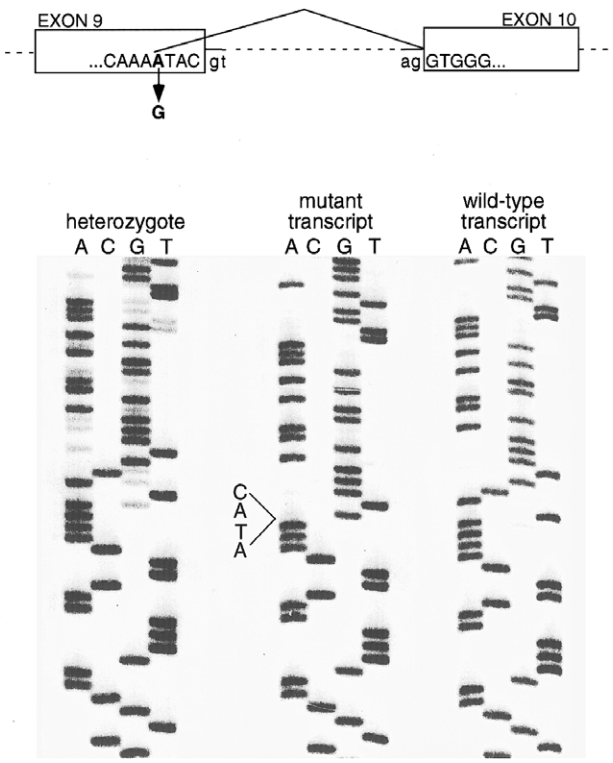

Figure 6 Aberrant splicing resulting from the 1367A→G mutation. *Top*, Schematic showing the position of the 1367A→G mutation in family 1676. *Bottom*, Sequencing-gel autoradiograph showing deletion of 4 nt at the 3′ end of exon 9 in the mutant transcript. Total RT-PCR product (heterozygote) or electrophoretically separated products (mutant and wild-type transcripts) are shown.

should have the same effects that we observed in neurons and other types of cells.

Both normal and mutant (deletion of exon 9) transcripts were produced from the IVS9+4A→G mutant allele in the RT-PCR analysis of patient-derived RNA. This led us to investigate whether some of the other mutations were also leaky. In analysis with an in vitro exon-trapping construct, none of the mutations appeared to be leaky, even IVS9+4A→G, which appeared to be leaky in vivo. Although this may be explained by differences between the cell types used in these distinct approaches, we surmised that it was instead due to differences in genomic sequence context—in particular, the strengths of the donor and acceptor splice-site sequences of adjacent exons. When we included additional genomic sequence including the endogenous splice junctions flanking the skipped exon, the leakiness of the IVS9+4A→G mutation was restored. We note that exon trapping and other minigene constructs commonly used in this type of analysis contain strong, viral-based donor and acceptor splice-site sequences within the vector, chosen for maximum splicing efficiency. These sequences could alter the effects of sequence variation that might affect splice-site selection. Thus, mutations that may be leaky in vivo may appear to be fully penetrant in the absence of extensive genomic-sequence context of the gene being investigated. Our findings suggest cau-

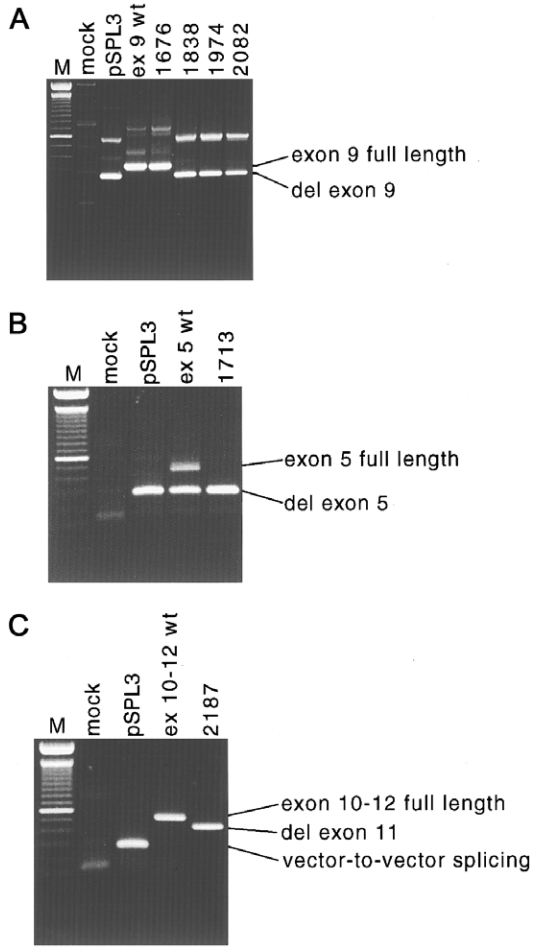

Figure 7 Effects of splice-site mutations on mRNA splicing in COS1 cells. The pSPL3 exon-trapping vector was used to assay splice-site selection. *A*, Cells were transfected with vector alone (lane pSPL3), or with wild-type exon 9 and flanking intronic sequence (lane ex 9 wt), or with the same construct but containing the mutations identified in the four families indicated (lanes 1676, 1838, 1974, and 2082). RT-PCR products were amplified with vector-specific primers. The mutations in families 1838, 1974, and 2082 cause skipping of exon 9; the mutation in family 1676 causes a 4-nt deletion from exon 9 (see fig. 6). *B*, Cells were transfected with vector alone (lane pSPL3), or with wild-type exon 5 and flanking intronic sequence (lane ex 5 wt), or with the same construct but containing the mutation identified in family 1713 (lane 1713). RT-PCR products were amplified with vector-specific primers. The mutation causes skipping of exon 5. *C*, Cells were transfected with vector alone (lane pSPL3), or with wild-type exons 10–12 and flanking intronic sequence (lane ex 10-12-wt), or with the same construct but containing the mutation identified in family 2187 (lane 2187). RT-PCR products were amplified with vector-specific primers. The mutation causes skipping of exon 11.

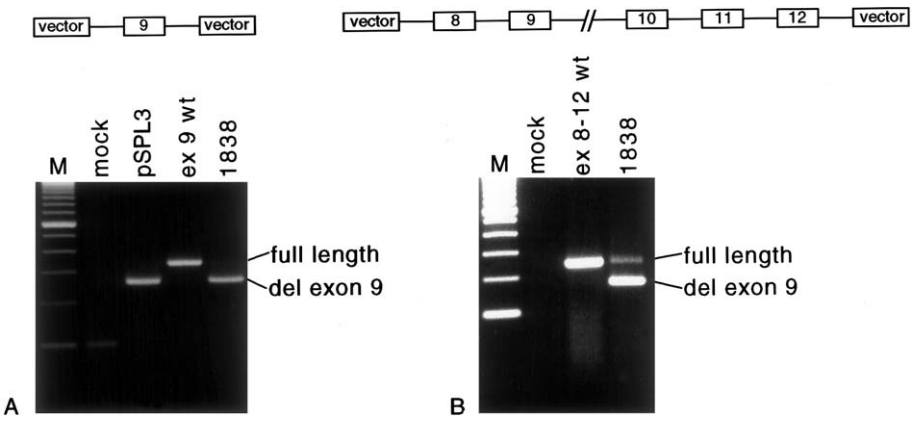

Figure 8 Differences in splice-site selection due to the IVS9+4A→G mutation depend on the extent of flanking genomic sequence context. The pSPL3 exon-trapping vector was used to assay splice-site selection. *A,* Cells were transfected with vector alone (lane pSPL3), or with wild-type exons 8–12 and flanking intronic sequence (lane ex 10-12-wt), or with the same construct but containing the mutation identified in family 1838 (lane 1838). RT-PCR products were amplified with vector-specific primers. In this minimal genomic sequence context, all transcripts produced from the mutant allele lack exon 9. *B,* Cells were transfected with wild-type exons 8–12 and flanking intronic sequence (lane ex 8-12 wt), or with the same transcript but containing the mutation identified in family 1838 (lane 1838). RT-PCR products were amplified with primers specific to exons 8 (forward primer) and 11 (reverse primer). In this more extensive genomic sequence context, the mutation is leaky. Both the full-length transcript and the transcript lacking exon 9 are produced from the mutant allele. The structures of the constructs used are shown at the top of each panel.

tion in the interpretation of data solely obtained with minigene constructs to study the effects of sequence variation on splicing.

The variable expressivity of SPG—and, in particular, that linked to *SPG4*—has been widely noted, to the extent that some earlier literature suggested anticipation for *SPG4*-linked families (Scott et al. 1997; McDermott et al. 2000). These suggestions have abated since the identification of inactivating spastin gene mutations, rather than a trinucleotide-repeat expansion; however, for the wide variability in phenotype, an account must still be made. If a model of haploinsufficiency for *SPG4*-linked SPG is assumed, the progression from normal function to disease state would appear to require a 50% reduction in spastin level. Our data, showing the production of normally spliced transcripts from at least one mutant spastin allele, suggest that the threshold of spastin required for this progression lies within a much narrower interval. Thus, relatively small differences in the level of wild-type spastin expression may have important functional consequences. Although the normal range of variability in spastin-expression level is unknown, in the context of a spastin-gene mutation—even a fully penetrant (i.e., nonleaky) mutation—such variability might be brought into a range in which it has dramatic phenotypic consequences. If the function of spastin is highly concentration dependent, consistent with the IVS9+4A→G mutation, the phenotype could vary in parallel with spastin levels. This may, at least in part, account for the wide ranges in age at onset, symptom severity, and rate of symptom progression that have been reported to occur in *SPG4*-linked SPG, both among and within families.

Acknowledgments

We thank the patients and their families for their participation. We thank Dr. Gregory J. Riggins (Duke University) for providing the sample of normal human brain. This work was supported in part by National Institutes of Health program project grant 2P01-NS26630-11A1.

Electronic-Database Information

The accession number and URLs for data in this article are as follows:

Genoscope Centre National de Séquençage, http://www.genoscope.cns.fr/externe/English/Projets/Projet_U/primers.html (for primer sequences) and http://www.genoscope.cns.fr/externe/English/Projets/Projet_U/cDNA.html (for spastin cDNA sequence)

Online Mendelian Inheritance in Man (OMIM), http://www.ncbi.nlm.nih.gov/Omim/ (for *SPG4* [MIM 182601])

References

Boehnke M (1986) Estimating the power of a proposed linkage study: a practical computer simulation approach. Am J Hum Genet 39:513–527

Bürger J, Fonknechten N, Hoeltzenbein M, Neumann L, Bratanoff E, Hazan J, Reis A (2000) Hereditary spastic paraplegia caused by mutations in the *SPG4* gene. Eur J Hum Genet 8:771–776

Fink JK (1997) Advances in hereditary spastic paraplegia. Curr Opin Neurol 10:313–318

Fonknechten N, Mavel D, Byrne P, Davoine C-S, Cruaud C, Boentsch D, Samson D, Coutinho P, Hutchinson M, McMonagle P, Burgunder J-M, Tartaglione A, Heinzlef O, Feki I, Deufel T, Parfrey N, Brice A, Fontaine B, Prud'homme J-F, Weissenbach J, Dürr A, Hazan J (2000) Spectrum of *SPG4* mutations in autosomal dominant spastic paraplegia. Hum Mol Genet 9:637–64

Fontaine B, Davoine C-S, Dürr A, Paternotte C, Feki I, Weissenbach J, Hazan J, Brice A (2000) A new locus for autosomal dominant pure spastic paraplegia, on chromosome 2q24-q34. Am J Hum Genet 66:702–707

Hazan J, Fonknechten N, Mavel D, Paternotte C, Samson D, Artiguenave F, Davoine C-S, Cruaud D, Dürr A, Wincker P, Brottier P, Cattolico L, Barbe V, Burgunder J-M, Prud'homme J-F, Brice A, Fontaine B, Heilig R, Weissenbach J (1999) Spastin, a new AAA protein, is altered in the most frequent form of autosomal dominant spastic paraplegia. Nat Genet 23:296–303

Hentati A, Deng H-X, Zhai H, Chen W, Yang Y, Hung W-Y, Azim AC, Bohlega S, Tandan R, Warner C, Laing NG, Cambi F, Mitsumoto H, Roos RP, Boustany R-M, Hamida MB, Hentati F, Siddique T (2000) Novel mutations in spastin gene and absence of correlation with age at onset of symptoms. Neurology 55:1388–1390

Körkkö J, Annunen S, Pihlajamaa T, Prockop DJ, Ala-Kokko L (1998) Conformation sensitive gel electrophoresis for simple and accurate detection of mutations: comparison with denaturing gradient gel electrophoresis and nucleotide sequencing. Proc Natl Acad Sci USA 95:1681–1685

Lindsey JC, Lusher ME, McDermott CJ, White KD, Reid E, Rubinsztein DC, Bashir R, Hazan J, Shaw PJ, Bushby KMD (2000) Mutation analysis of the spastin gene (*SPG4*) in patients with hereditary spastic paraplegia. J Med Genet 37: 759–765

McDermott CJ, White K, Bushby K, Shaw PJ (2000) Hereditary spastic paraparesis: a review of new developments. J Neurol Neurosurg Psychiatry 69:150–160

Neuwald AF, Aravind L, Spouge JL, Koonin EV (1999) AAA^{+}: a class of chaperone-like ATPases associated with the assembly, operation, and disassembly of protein complexes. Genome Res 9:27–43

Patel S, Latterich M (1998) The AAA team: related ATPases with diverse functions. Trends Cell Biol 8:65–71

Ploughman LM and Boehnke M (1989) Estimating the power of a proposed linkage study for a complex genetic trait. Am J Hum Genet 44:543–551

Reid E, Dearlove AM, Osborn O, Rogers MT, Rubinsztein DC (2000) A locus for autosomal dominant "pure" hereditary spastic paraplegia maps to chromosome 19q13. Am J Hum Genet 66:728–732

Santorelli FM, Patrono C, Fortini D, Tessa A, Comanducci G, Bertini E, Pierallini A, Amabile GA, Casali C (2000) Intrafamilial variability in hereditary spastic paraplegia associated with an *SPG4* gene mutation. Neurology 55:702–705

Scott WK, Gaskell PC, Lennon F, Wolpert CM, Menold MM, Aylsworth AS, Warner C, Farrell CD, Boustany R-MN, Albright SG, Boyd E, Kingston HM, Cumming WJK, Vance JM, Pericak-Vance MA (1997) Locus heterogeneity, anticipation and reduction of the chromosome 2p minimal candidate region in autosomal dominant familial spastic paraplegia. Neurogenetics 1:95–102